Published in final edited form as:
Stem Cells. 2008 April ; 26(4): 864–873. doi:10.1634/stemcells.2007-0843.

Comparison of Reporter Gene and Iron Particle Labeling for Tracking Fate of Human Embryonic Stem Cells and Differentiated Endothelial Cells in Living Subjects

Zongjin Li[1], **Yoriyasu Suzuki**[2], **Mei Huang**[1], **Feng Cao**[1], **Xiaoyan Xie**[1], **Andrew J. Connolly**[3], **Phillip C. Yang**[2], and **Joseph C. Wu**[1,2]

[1]Department of Radiology and Molecular Imaging Program at Stanford (MIPS), Stanford University School of Medicine, Stanford, CA, USA

[2]Department of Medicine, Division of Cardiology, Stanford University School of Medicine, Stanford, CA, USA

[3]Department of Pathology, Stanford University School of Medicine, Stanford, CA, USA

Abstract

Human embryonic stem (hES) cells are pluripotent stem cells capable of self-renewal and differentiation into virtually all cell types. Thus, they hold tremendous potential as cell sources for regenerative therapies. The concurrent development of accurate, sensitive, and noninvasive technologies capable of monitoring hES cells engraftment *in vivo* can greatly expedite basic research prior to future clinical translation. In this study, hES cells were stably transduced with a lentiviral vector carrying a novel double-fusion reporter gene that consists of firefly luciferase and enhanced green fluorescence protein (Fluc-eGFP). Reporter gene expression had no adverse effects on cell viability, proliferation, or differentiation to endothelial cells (hESC-ECs). To compare the two popular imaging modalities, hES cells and hESC-ECs were then co-labeled with superparamagnetic iron oxide (SPIO) particles before transplantation into murine hindlimbs. Longitudinal magnetic resonance (MR) imaging showed persistent MR signals in both cell populations that lasted up to 4 weeks. By contrast, bioluminescence imaging indicated *divergent* signal patterns for hES cells and hESC-ECs. In particular, hESC-ECs showed significant bioluminescence signals at day 2, which decreased progressively over the following 4 weeks, whereas bioluminescence signals from undifferentiated hES cells increased dramatically during the same period. Postmortem histology and immunohistochemistry confirmed teratoma formation after injection of undifferentiated hES cells, but not hESC-ECs. Taken together, we conclude that reporter gene is a better marker for monitoring cell viability, whereas iron particle labeling is a better marker for high-resolution detection of cell location by MR. Furthermore, transplantation of pre-differentiated rather than undifferentiated hES cells would be more suited for avoiding teratoma formation.

Keywords

MRI; Bioluminescence Imaging; Human Embryonic Stem Cells; Endothelial Cells; Differentiation; Teratoma Formation; Acute Donor Cell Death

Correspondence to: Joseph C. Wu, MD, PhD, Stanford University School of Medicine, Edwards Building, R354, Stanford, CA 94305-5344, Ph: 650-736-2246, Fax: 650-736-0234, joewu@stanford.edu.

INTRODUCTION

Human embryonic stem (hES) cells are derived from the inner cell mass of pre-implanted blastocysts [1]. They have been shown to differentiate into a variety of cell types that represent endoderm, ectoderm, and mesoderm origins via three-dimensional structures called embryoid bodies (EBs), which at least partially mimic the spatial organization of the embryo [1–4]. Various lineages have been derived from hES cells, including neurons [5], cardiomyocytes [6, 7], hematopoietic cells [8, 9], osteogenic cells [10], hepatocytes [11], insulin-producing cells [12], keratinocytes [13] and endothelial cells [3, 4, 14]. Furthermore, these cells appear to be weakly immunogenic, with absent MHC-II and only low levels of MHC-I molecules [15]. Given their unlimited self-renewal and pluripotency capacity, hES cells represent a new and exciting avenue for stem cell therapy. In cell culture, hES cells can differentiate into endothelial cells through successive maturation steps [4, 9, 16]. Therefore, the isolation and use of hES-derived endothelial cells (hESC-ECs) have potential therapeutic applications, including cell transplantation for repair of ischemic tissues and tissue-engineered vascular grafts.

Stem cell therapy is an exciting area of research that promises future treatment of many diseases [17]. However, to fully understand the beneficial effects of stem cell therapy, investigators must be able to track the biology and physiology of transplanted cells in *living* subjects over time. At present, most cell therapy protocols require histological analysis to determine viable engraftment of the transplanted cells. The development of sensitive, noninvasive technologies to monitor this fundamental engraftment parameter will greatly aid clinical implementation of cell therapy. In reporter gene imaging, stem cells can be genetically engineered to express various reporter genes before transplantation. The reporter genes can be detected by sensitive imaging devices such as the optical coupled device (CCD), single photon emission computed tomography (SPECT), or positron emission tomography (PET) [18]. Magnetic resonance (MR) imaging of stem cells is also an emerging application for monitoring cell engraftment. In particular, stem cells labeled with superparamagnetic iron oxide (SPIO) particles can be identified *in vivo* as hypointensities in MR images, as the iron shortens transverse proton relaxation times. The spatial and temporal resolution of MR imaging allow the location of iron-labeled donor cells to be monitored noninvasively over several weeks *in vivo* [19–21]. A fundamental drawback of hypointense signal is the difficulty in distinguishing iron-labeled cells from the surrounding air, hemorrhage, necrosis, and macrophages. To address these problems, techniques to generate positive contrast to enhance signal- and contrast-to-noise ratios of the iron-labeled stem cells have been developed. Cunningham *et al.* have reported off-resonance (OR) MR imaging of iron-labeled *mouse* ES cells to generate positive contrasts through suppression of background tissue [22]. However, whether these different methodologies can be applied for studying the engraftment of hES cells and their derivatives *in vivo* has yet to be examined. To help answer these important questions, we performed a head-to-head comparison of tracking undifferentiated hES cells and differentiated hESC-ECs using reporter gene and iron particle imaging.

MATERIALS AND METHODS

Maintenance and differentiation of human embryonic stem cells

Undifferentiated hES cells (H9 line from Wicell, passages 35 to 45) were grown on an inactivated mouse embryonic fibroblast (MEF) feeder layer as previously described [9]. Briefly, the cell was maintained at an undifferentiated stage on irradiated low-passage MEF feeder layers on 0.1% gelatin-coated plates. The medium was changed daily. The medium consisted of Dulbecco's modified Eagle's medium (DMEM)/F-12, 20% knockout serum replacement, 0.1 mM nonessential amino acids, 2 mM L-glutamine, 0.1 mM β-

mercaptoethanol, and 4 ng/ml rhFGF-2 (R&D Systems Inc., Minneapolis). The undifferentiated hES cells were treated by 1 mg/ml collagenase type IV in DMEM/F12 and scraped mechanically on the day of passage. Prior to iron labeling and endothelial differentiation, hES cell were seeded onto Matrigel-coated plates in conditioned medium (CM) prepared from MEF as follows [23]. MEF cells were harvested and irradiated with 50 Gy, and cultured with hES medium without bFGF. CM was collected daily and supplemented with an additional 4 ng/ml of bFGF before feeding hES cells.

In vitro differentiation of hESC-ECs

To induce hES cell differentiation, undifferentiated hES cells were cultured in differentiation medium containing Iscove's modified Dulbecco's medium (IMDM) and 15% defined fetal bovine serum (FBS) (Hyclone, Logan, UT), 0.1 mM nonessential amino acids, 2 mM L-glutamine, 450 μM monothioglycerol (Sigma, St. Louis, MO), 50 U/ml penicillin, and 50μg/ml streptomycin, either in ultra-low attachment plates for the formation of suspended embryoid bodies (EBs) as previously described [4, 9]. Briefly, hES cells cultured on Matrigel coated plate with CM were treated by 2 mg/ml dispase (Invitrogen, Carlsbad, CA) for 15 minutes at 37°C to loosen the colonies. The colonies were then scraped off, and transferred into ultra low-attachment plates (Corning Incorporated, Corning, NY) for EB formation.

Whole-mount immunostaining of human embryoid bodies (hEBs)

Whole-mount immunohistostaining of hEBs was performed as previously described [3] with minor modifications. The hEBs were fixed in methanol and DMSO (4:1) at 4°C overnight. For staining, the rehydrated hEBs were first blocked by two incubations in PBSBT (2% BSA and 0.2% Tween-20 in PBS), then with PBSBT containing mouse anti-human MoAb CD31 (Becton Dickinson) overnight at 4°C. The hEBs were washed five times in PBSBT each for 1 h at 4°C for the initial three washes and at room temperature for final two. The primary antibody was labeled by incubating the hEBs with Alex 594-conjugated goat anti-mouse IgG (Invitrogen) in PBSBT overnight at 4°C and nuclear counterstained with DAPI.

Flow cytometry sorting (FCS) of hESC-ECs

Single cell suspensions from day 12 of differentiated hEBs were obtained by treatment with 0.56 units/ml of Liberase Blendzyme IV (Roche, Indianapolis) at 37°C for 20–30 min. Cells were passed through a 40-μm cell strainer [7]. Cells were incubated for 30 min at 4°C with mouse phycoerythrin (PE) conjugated anti-human CD31 (BD). The $CD31^+$ cells were isolated using FACScan (Becton Dickinson). To generate hESC-ECs, the isolated $CD31^+$ cells were grown on 0.1% gelatin or 4 $\mu g/cm^2$ human fibronectin (Calbiochem, San Diego, CA) coated plates in EGM-2 with 5% FBS. The medium was changed every 2–3 days.

Biological characteristics of hESC-ECs

Flow cytometry analysis, DiI-ac-LDL uptake assay, and Matrigel assay were used to confirm endothelial cell phenotype within these $CD31^+$ purified hES cells. Antibodies used in this study were phycoerythrin (PE) conjugated anti-CD31 (BD Pharmingen) and Allophycocyanin (APC) conjugated anti-KDR (R&D Systems), APC conjugated anti-mouse IgG2a, and mouse anti-human VE-cadherin (BD Pharmingen). The stained cells were analyzed using FACS Vantage (Becton-Dickinson, MA). Dead cells stained by propidium-iodide (PI) were excluded from the analysis. Isotype-identical antibodies served as controls (BD Pharmingen). Approximately 5×10^5 undifferentiated hES cells and 2×10^5 differentiated hESC-ECs were used to run the FACS. ForDiI-ac-LDL uptake assay, hESC-ECs were incubated with 10 μg/ml of DiI-Ac-LDL (Molecular Probes, Eugene, OR) at 37°C for 6 hours. After washing with PBS twice, the slides were fixed and counterstained with DAPI

(4, 6-diamidino-2-phenylindole), mounted with mounting medium (Vector Laboratories, Burlingame, CA), and covered with coverslips prior to detection with fluorescence microscopy as described [9]. The formation of endothelial tubes was assessed by seeding cells in 24-well plates coated with Matrigel (BD Pharmingen) and incubating them at 37° for 12 hours as described [14, 24].

Real time RT-PCR (qRT-PCR)

qRT-PCR assays were performed using the human endothelial cell biology RT^2 Profiler™ PCR Array (SuperArray Bioscience, Frederick, MD) on an ABI PRISM 7900 HT (Applied Biosystems, Foster City, CA). Data analysis are available at the company website (http://www.superarray.com/pcr/arrayanalysis.php). Briefly, total RNAs were isolated using RNeasy (Qiagen, Waltham, MA) from undifferentiated hES cells at day 0, differentiated hEBs at day 12, hESC-derived endothelial cells (after CD31 sort), and human umbilical endothelial cells (HUVEC) as positive control. First-strand cDNAs were generated using iScript Select cDNA Synthesis Kit (BioRad, Hercules, CA). For real-time PCR reaction, first-strand cDNAs were added to RT qPCR Master Mix (SuperArray Bioscience). Samples were heated for 10 min at 95°C and then subjected to 40 cycles of denaturation at 95°C for 15 sec and annealing and elongation at 60°C for 1 min. Methods for conventional RT-PCR analysis and primer sequences for endothelial specific genes (CD31, VE-cadherin, KDR, Oct-4, GAPDH) are described in Supplemental Methods and Supplemental Table, respectively.

Lentiviral transduction of hES cells with double fusion (DF) reporter gene

In order to track transplanted cells *in vivo*, hES cells were transduced at multiplicity of infection (MOI) of 10 with self-inactivating (SIN) lentiviral vector carrying a human ubiquitin promoter driving firefly luciferase and enhanced green fluorescence protein (Fluc-eGFP). Stable clones were isolated using FACS for eGFP expression. Afterwards, Fluc activity within different cell numbers was confirmed *ex vivo* using Xenogen IVIS 200 system (Xenogen, Alameda, CA) as described [18]. Non-transduced hES cells (control) and hES cells with DF reporter gene (hESC-DF) were stained for Oct-4 (Chemicon, Temecula, CA). The undifferentiated hES cell colonies were fixed in 4% paraformaldehyde in PBS for 15 minutes. Nonspecific binding was blocked with 4% normal goat serum for 30 minutes, following which the colonies were stained with antibodies to Oct-4 and incubated with Alexa 594-conjugated rabbit anti-goat secondary antibodies (Invitrogen) for 30 minutes and nuclear counterstained with DAPI. Images were obtained with a Zeiss Axiovert microscopy (Sutter Instrument Co., USA). Subsequently, the processes for *in vitro* endothelial cell differentiation and characterization were the same as control non-transduced hES cells described earlier.

Labeling of hES cells and hESC-ECs with iron particles

Transduced hES cells and derived hESC-ECs were labeled with Feridex IV-protamine sulfate (FE-Pro) as described [25] with minor modifications. The commercially available superparamagnetic iron oxide (SPIO) suspension, (Feridex IV®, Berlex Laboratories, Inc, Wayne, NJ) contains particles approximately 80–150 nm in size and has a total iron content of 11.2 mg/ml. Preservative-free protamine sulfate (American Pharmaceuticals Partner Inc., Schaumburg, IL), 10 mg/ml, was prepared as a fresh stock solution of 1 mg/ml in distilled water at the time of use. SPIO at a concentration of 100 μg/ml was put into a mixing tube containing serum-free culture medium. Protamine sulfate (12 μg/ml) was added and the entire suspension was mixed for 5–10 minutes. The final FE-Pro suspension was added directly to the existing medium, incubated overnight. The final concentration of Feridex IV and protamine sulfate was 50 μg/ml and 6 μg/ml of medium, respectively. After overnight incubation, the hES cells and hESC-ECs were washed twice with phosphate-buffered saline

(PBS), and harvested by treating with collagenase IV and trypsin, respectively. Next, the trypan blue exclusion assay was used to assess viability and cytotoxicity of iron labeling on hES cells and hESC-ECs. Six samples were performed and averaged for these assays.

Transplantation of hES cells and hESC-ECs into murine hindlimbs

All procedures were performed on 8–10 week old female SCID beige mice (Charles River Laboratories, Inc.) (n=15) according to the Stanford University Animal Care and Use Committee guidelines. Mice were anesthetized with inhaled isoflurane (2% to 3%). Approximately 1×10^6 undifferentiated hES cells and 1×10^6 hESC-ECs (both stably transduced with DF reporter gene and co-labeled with SPIO particles) were injected into right and left hind limbs of the same mouse, respectively, in 100μl PBS.

Optical bioluminescence imaging of transplanted cell fate in living mice

Bioluminescence imaging was performed using the Xenogen IVIS 200 system. After intraperitoneal injections of reporter probe D-Luciferin (150 mg luciferin/kg), animals were imaged for 2 seconds to 2 minutes. The same mice were scanned for 4 weeks. Imaging signals were quantified in units of maximum photons per second per centimeter square per steridian (photons/sec/cm^2/sr) as described [18]. Bioluminescence imaging was performed by an investigator blinded to the study conditions (XX).

MR imaging of transplanted cell fate in living mice

Afterwards, *in vivo* MR imaging was performed on the 1.5 T-MR scanner (Signa, GE Medical Systems, Milwaukee, WI) using a 3-inch surface coil. The mice were anesthetized with intraperitoneal injection of ketamine (100 mg/kg) and xylazine (20 mg/kg) and imaged in a prone position. After 3D-plane localization, images were acquired in a coronal plane using gradient-recalled echo (GRE) sequence (TR = 100msec, TE = 10msec, Flip angle = 30°, FOV = 8×8cm, slice thickness = 1 mm, slice gap = 0 mm, matrix = 256×256, NEX = 4). Multiple contiguous coronal slices consisting of 9–10 slices were acquired for complete coverage of the mice hind limb. Following GRE, Off-Resonance (OR) sequence was applied to the transplanted labeled cells. Briefly, OR utilizes spectrally selective radiofrequency (RF) pulses to excite and refocus the off-resonance water surrounding the labeled cells while suppressing on-resonance signal. This generates positive contrast from the hydrogen protons adjacent to the labeled cells and helps identify and estimate the volume of the labeled cells [22]. Projectional OR imaging was performed with TR = 800 msec, TE = 14msec, FOV = 20 cm, and matrix = 256×128 with 2 discrete Fourier transformation (DFT) encoding and an 8-ms readout [22]. Measurement of signals in the region of interest (ROI) was performed with the Image J software. The signal volume of GRE images was measured by summation of hypointense area of each slice. The OR signal enhancement area was obtained by measuring the area of projectional OR image. MR imaging was performed by an investigator blinded to the study condition (YS). Protocol for *ex vivo* MR imaging of cell suspension is included in the Supplementary Methods.

Immunohistochemical staining for macrophages, iron particles, and various cell types

Mice were euthanized at four weeks after cell transplantation. Both hind limbs were embedded in paraffin and cut into 5 μm sections. H&E and Prussian staining were carried out to identify the fate of transplanted hES cells and hESC-ECs doubly labeled with iron particles and reporter genes. To examine whether the iron particles are localized in the macrophages, staining of macrophages (Mac-3) and iron particles were performed. Sections were first incubated with the monoclonal rat anti-mouse macrophage Mac-3 antibody (BD Parmingen) for one hour and then with a second antibody, biotinylated goat anti-rat secondary antibody (Invitrogen), for another hour. Streptavidin-horseradish peroxidase

(HRP) was then applied for 30 minutes and HRP activity was detected by with 3,3′-Diaminobenzidine (DAB). For iron particle staining, sections were incubated with Perls reagent in the dark for 30 minutes and counterstained with fast red. For immunofluorescence histology, both hind limbs were embedded into OCT compound (Miles Scientific, Elkhart, IN) and 5μm frozen sections were cut. For immunostaining, sections were incubated with primary antibodies, rat anti-mouse macrophage Mac-3 antibody (BD Pharmingen), rabbit anti-GFP (Invitrogen), and goat anti-mouse CD31 (Santa Cruz Biotechnology), followed by incubation with secondary antibody, APC-conjugated mouse anti-rat IgG (BD Pharmingen), Alex 488 conjugated donkey anti-rabbit IgG (Invitrogen), Alex 594 conjugated donkey anti-goat IgG (Invitrogen), then counter stained with DAPI. Histologic interpretation was performed by a pathologist blinded to the study conditions (AJC).

Statistical Analysis

ANOVA and repeated measures ANOVA with post-hoc testing as well as the two-tailed Student's *t*–test were used. Differences were considered significant at *P*-values of <0.05. Unless otherwise specified, data are expressed as mean ± standard deviation.

RESULTS

Characterization and differentiation of hES cells

In order to compare the fate of undifferentiated versus differentiated hES cells *in vivo*, we first established a differentiation protocol to induce hESC-ECs (Figure 1A). Undifferentiated hES cell (H9 line) were maintained either on irradiated MEF feeder cells or on Matrigel coated plates in the presence of MEF condition medium [9]. To isolate endothelial cells from hES cells, undifferentiated hES cells cultured on Matrigel coated plated were placed into Petri dishes with differentiation medium for induction of EB formation. Previous studies have shown that differentiated hEBs from hES cells contain endothelial cells which can be isolated by CD31 [4] or CD34 markers [9]. In this study, whole-mount immunostaining confirmed that within day-12 hEBs, the $CD31^+$ endothelial cells were organized in specific channel-like structures (Figure 1B). These data confirm that hES cells cultivated as hEBs spontaneously differentiated to endothelial cells and formed blood vessel-like structures. Initial FACS analysis showed that ~3% cells expressed CD31 marker. This population of $CD31^+$ was sorted, cultured, and propagated for further analysis to confirm endothelial cell traits. In particular, we examined CD31, VE-cadherin, and KDR, which are known to be markers for endothelial differentiation of ES cells [3, 4, 9, 26, 27]. As expected, both FACS and quantitative RT-PCR analysis indicated undifferentiated hES cells expressed endothelial markers at low level. After endothelial induction, ICAM1, CD31, VCAM1, vWF, and VE-cadherin were upregulated while Oct-4 expression (marker for undifferentiated state) was downregulated (Figures 1C, 1D & Supplemental Figure 1A). Quantitative RT-PCR analysis showed similar endothelial gene expression pattern of hES-ECs compared to HUVECs but great disparity between hESC-ECs and hES cells (Figure 1D & Supplemental Figures 1B & 1C). Interestingly, KDR was continuously expressed in both undifferentiated and differentiated hES cells as shown by RT-PCR and FACS (Figures 1C & 1D, Supplemental Figure 1A). This pattern of expression is unlike mouse ES cells whereby KDR is specifically expressed on hemagioblasts but not on undifferentiated ES cells [3]. After 1 week of culturing, flow cytometry was again performed using antibodies directed against endothelial markers such as VE-cadherin and CD31. Isolated cells continued to express robust levels of both VE-cadherin and CD31 (>80%). These CD31 cells morphologically resembled HUVECs and can form tube-like structure on Matrigel (Figure 1E).

Genetic labeling of hES cells with double fusion (DF) reporter gene

In order to develop an imaging platform for tracking transplanted hES cells and hESC-ECs in living animals, we used a DF reporter gene consisting of Fluc-eGFP (Figure 2A). The efficiency of self-inactivating lentiviral vector for transducing hES cells was ~20% (data not show). Both control non-transduced hES cells and stably transduced hES cells showed similar expression patterns of stem cell markers Oct-4 on immunostaining, suggesting minimal side effects by reporter gene on maintaining stem cell state (Figure 2B). Upon culturing onto 24-well plates, we also observed a strong correlation (r^2=0.99) between Fluc activity and cell numbers *ex vivo* using the Xenogen IVIS system (Figure 2C). The cell proliferation and cell viability data are also similar between control hES cells and transduced hES cells (data not shown). Overall, these data are consistent with our previous studies showing minimal effects of reporter genes on mouse ES cell survival, proliferation, and differentiation [18, 28, 29]. In addition, the differentiation procedure and differentiation efficiency of stably transduced hES cells were similar to control non-transduced hES cells. Isolated cells express robust levels of both VE-cadherin and CD31, and avidly incorporate DiI-ac-LDL (Figure 2D & 2E). Uptake of DiI-ac-LDL has been used to characterize mature endothelial cells [30]. The isolated cells similarly can form tube-like structure on Matrigel (data not shown). Overall, reporter gene expression did not seem to significantly affect the typical characteristics of endothelial cells as measured by immunostainings, DiI-ac-LDL uptake, and Matrigel angiogenesis assay.

Physical labeling of hES cells with iron particle

In order to track transplanted cells using MR imaging *in vivo*, hES cells and hESC-ECs (both stably expressing the DF reporter gene) were co-labeled with iron particles. After staining with Prussian Blue, iron labeled cells were found to have cytosolic accumulation of iron. Interestingly, the iron uptake of hES cells was less than hESC-ECs, which is likely due to difference in their physical size (Figure 3A). Similarly, *in vitro* cellular MR imaging demonstrated that dephasing signals in hES cells were weaker than those in hESC-ECs. Representative *in vitro* cellular MRI of labeled cells is shown in Figure 3B. Finally, the cell viability assay showed no significant difference between control unlabeled hES cells versus iron particle labeled hES cells (Figure 3C).

Longitudinal MR imaging of hES cell survival in living animals

In order to evaluate whether MR imaging can be used to serially monitor cell survival following transplantation, we injected 1×10^6 iron-labeled hES cells into left hind limbs and 1×10^6 iron-labeled hESC-ECs into right hind limbs of SCID beige mice. We then imaged these iron-labeled cells repetitively for up to 4 weeks. Representative serial MR images of iron-labeled cells by GRE and OR [22] sequences during the 4-week period are shown in Figures 4A and 4C, respectively. Control animals injected with *unlabeled* cells showed no MR signals as expected. Similar to the *in vitro* data showing more cytosolic accumulation of iron particles within the larger size hESC-ECs (Figure 3A), we noted the GRE and OR signals were also stronger in the right (hESC-ECs) compared to left (hESC) hind limbs. Four week after cell transplantation, MR imaging with GRE sequence showed a significant increase in the *physical size* of the left hind limb injected with iron-labeled hES cells, which is due to teratoma formation (Figure 4A). However, when normalized to day 2, analysis of both MR imaging signals (GRE and OR) produced no difference at 4 weeks as shown in Figures 4B and 4D (P=0.001).

Longitudinal reporter gene imaging of hES cell survival in living animals

Since the same animals described above were injected with hES cells and hESC-ECs double labeled with iron particles and Fluc-eGFP, we decided to analyze the ability of reporter gene

imaging for assessing stem cell fate (e.g., engraftment, proliferation, and death). Longitudinal bioluminescence imaging was also performed in the same animals for 4 weeks (Figure 5A). In both hind limbs, bioluminescence signals were most robust immediately after transplantation (day 2). In the hESC-EC group, bioluminescence signals progressively decreased from day 2 to day 28 (P=0.001 vs. control for all time points), indicating acute donor cell loss. Control animals injected with PBS showed no imaging signals as expected. Quantitative analysis shows that the hESC-ECs survival activity at day 21 was less than 1.5% compared to day 2. This survival pattern of *differentiated* hESC-ECs is markedly different when compared to *undifferentiated* hES cells, which was >40-fold higher compared to day 2 (Figure 5B). Interestingly, the undifferentiated hES cell survival activity decreased to about 25% baseline from day 2 to day 7, followed by a robust rebound of cell survival activity from day 14 to day 28. This dichotomous pattern of hES cell death followed by hES cell proliferation was seen in most animals analyzed.

Postmortem histology and immunohistochemistry

In order to confirm our *in vivo* imaging data (both MR and bioluminescence), all animals were sacrificed 4 weeks after cell transplantation. Teratoma formation was observed uniformly within the left hind limbs injected with undifferentiated hES cells (Supplement Figure 2A), but *not* in the right hind limbs injected with differentiated hESC-ECs. Immunostaining for macrophages (Mac-3) reveals that in the right hind limbs injected with hESC-ECs, most of the iron particles were deposited between muscle bundles and taken up by macrophages, thus accounting for the persistent MR signals seen at 4 weeks (Figure 6A). Immunofluorescence staining showed similar macrophage deposition pattern and GFP^+ hESC-ECs were seldom found but few integrated into host microvasculatures (Figure 6B, Supplement Figure 2B). In the left hind limbs injected with undifferentiated hES cells, macrophage infiltration was distributed between muscle fibers. As expected, the teratoma formation stained GFP^+ uniformly throughout (Figures 6C & 6D). The unique morphology of hES cells, which are round and small with relatively large nuclei, make them easily identifiable from the surrounding muscle.

DISCUSSION

The main aims of this study were to identify suitable molecular markers for serial monitoring of hES cell survival following transplantation and to compare the *in vivo* behavior of differentiated versus undifferentiated hES cells. Here for the first time we have compared the use of two popular cell markers, Fluc reporter gene and SPIO MR contrast agent, for labeling hES cells and their derived endothelial cells *ex vivo.* Under proper differentiation conditions, hES cells can be differentiated into functional endothelial cells, which express high levels of CD31 and VE-cadherin and can form tube-like structures on Matrigel assay and uptake DiI-ac-LDL. After double labeling, the fate of transplanted hES cells and hESC-ECs can be monitored by both imaging techniques. For bioluminescence imaging, a time-dependent decrease of cell signal activity was observed in the hESC-EC group, indicating significant acute donor cell loss. By contrast, engraftment of undifferentiated hES cells was followed by dramatic increases in bioluminescence signals from week 2 to week 4, which were confirmed as teratoma formation by postmortem analysis. For MR imaging, persistent and stable signals (both GRE and OR) were seen within both hind limbs injected with undifferentiated hES cells and differentiated hESC-ECs. The negative contrast GRE sequence of MR revealed higher anatomic resolution of the teratoma formation, and the positive contrast OR sequence readily showed the cell location after injection. However, overall MR imaging was *unable* to distinguish cell viability from cell proliferation as its signals remained relatively constant over the 4 week time span.

MRI has been used for tracking mouse ES cells [31] and mesenchymal stem cells [21, 32, 33] in the heart and brain. However, in this study, MR imaging demonstrated *stable* signals in both hind limbs implanted with undifferentiated hES cells and undifferentiated hESC-ECs over 4 weeks. Thus, MR imaging was unable to specifically distinguish viable from non-viable cells or proliferating from non-proliferating cell populations. This is not surprising because, as the cells proliferate, the constant number of SPIO nanoparticles is merely divided among the daughter cells [19, 20]. Moreover, the iron from cells undergoing apoptosis or cell lyses can be internalized by resident macrophages or remain in the local tissue. Altogether, these findings suggest that MR imaging, at least in the way utilized in this study, cannot distinguish iron-labeled cells from free iron released upon cell death, making iron labeling a less suitable marker for tracking long-term cell survival. Finally, the divergent pattern of survival (hESC-ECs vs. hES cells) seen in our reporter gene data are also consistent with previous studies showing poor donor cell survival after adult stem cell transplantation and uncontrolled teratoma formation after introduction of undifferentiated ES cells [14, 18, 34, 35].

For bioluminescence imaging, several studies have found a close relationship between cell numbers and imaging signals [14, 18, 34, 36]. In this study, we were able to determine the kinetics of hES cell and hESC-EC survival over time. By imaging the same individual animal, we avoided the sampling biases and errors that bedevil conventional studies in which groups of animals have to be sacrificed at different time points for histology purpose [36]. Nevertheless, at present bioluminescence imaging still lacks adequate tomographic resolution (Figure 5) due to attenuation of photons within tissues. To solve this problem, a combined multi-modality approach (e.g., bioluminescence imaging with MR or PET) may be designed in the future as a more suitable approach to monitor the *spatial* and *temporal* kinetics of transplanted hES donor cells in animal models *in vivo*.

Human ES cells are remarkable for their unlimited self-renewal and pluripotency capacity, making them highly desirable candidates for cell replacement therapy [1]. One major risk involving the use of hES cells, however, is the possibility of cell misbehavior following trasnplantation. This potentially serious complication may occur if any of the transplanted undifferentiated ES cells take on teratoma formation [14, 18]. In our study, the survival kinetics of undifferentiated hES cells was different compared to pre-differentiated hESC-ECs, with acute donor cell loss from day 2 to day 14 followed by a strong rebound of cell survival and proliferation from week 2 to week 4 due to subsequent teratoma formation. Thus, the ability to visualize cellular proliferation and differentiation *in vivo* in both pre-differentiated and undifferentiated populations would be of great benefit in monitoring cellular behavior. On the other hand, endothelial cells are promising key factors for the repair of ischemic tissues and formation of new blood vessels [2, 37, 38]. Several studies have explored the endothelial potential of hES cells, mainly by demonstrating the spontaneous differentiation of EBs to vascular-like structures and isolating hESC-ECs [4, 9, 16]. In this study, hESC-ECs isolated from hEBs after 12 days of differentiation displayed characteristics similar to vascular endothelium and expressed typical EC markers similar to those expressed in HUVECs such as VE-cadherin, CD31 and Dil-ac-LDL uptake. However, bioluminescence imaging data suggest that by week 4, <1.5% of the transplanted hESC-ECs are still alive. This observation conforms with other studies showing poor donor cell survival using serial histology, TUNEL apoptosis assay, or Taqman *Sry* PCR techniques [35]. Thus, the application of bioengineering methods or pro-survival cocktails [39], rather than direct stem cell injection, may prove to be a more viable approach for achieving long-term engraftment in the future [37].

In conclusion, though pluripotent hES cells represent a potentially unlimited source of cells for regeneration medicine, teratoma formation observed in this study and other reports [14,

18] recommends that extreme caution be exercised. Careful and precise protocols for acquiring differentiated cells are needed. To confirm the fate of hES cells *in vivo*, it is crucial to continue the development and further refinement of noninvasive imaging techniques. To that end, we compared the effects of labeling hES cells with reporter gene and iron particles. We showed that MR signals were persistent over a span of 4 weeks regardless of imaging undifferentiated hES cells (leads to teratoma formation) or differentiated hESC-ECs (leads to acute donor cell death). These data lead us to believe that reporter gene imaging is a better technique for monitoring long-term cell viability, death, and proliferation, while MR imaging is a better technique for high-resolution detection of cell location post transplantation.

Supplementary Material

Refer to Web version on PubMed Central for supplementary material.

Acknowledgments

This work was supported in part by grants from the NIH HL074883, NIH HL089027, BWF Career Award in Biomedical Sciences, and AHA BGIA (JCW) as well as the Stanford Dean's Fellowship (ZL).

References

1. Thomson JA, et al. Embryonic stem cell lines derived from human blastocysts. Science. 1998; 282(5391):1145–7. [PubMed: 9804556]
2. Levenberg S, et al. Endothelial potential of human embryonic stem cells. Blood. 2007; 110(3):806–14. [PubMed: 17412888]
3. Li ZJ, et al. Kinetic expression of platelet endothelial cell adhesion molecule-1 (PECAM-1/CD31) during embryonic stem cell differentiation. J Cell Biochem. 2005; 95(3):559–70. [PubMed: 15786495]
4. Levenberg S, et al. Endothelial cells derived from human embryonic stem cells. Proc Natl Acad Sci U S A. 2002; 99(7):4391–6. [PubMed: 11917100]
5. Reubinoff BE, et al. Neural progenitors from human embryonic stem cells. Nat Biotechnol. 2001; 19(12):1134–40. [PubMed: 11731782]
6. Xu C, et al. Characterization and enrichment of cardiomyocytes derived from human embryonic stem cells. Circ Res. 2002; 91(6):501–8. [PubMed: 12242268]
7. Xu C, et al. Human embryonic stem cell-derived cardiomyocytes can be maintained in defined medium without serum. Stem Cells Dev. 2006; 15(6):931–41. [PubMed: 17253954]
8. Kaufman DS, et al. Hematopoietic colony-forming cells derived from human embryonic stem cells. Proc Natl Acad Sci U S A. 2001; 98(19):10716–21. [PubMed: 11535826]
9. Chen T, et al. Stromal cell-derived factor-1/CXCR4 signaling modifies the capillary-like organization of human embryonic stem cell-derived endothelium in vitro. Stem Cells. 2007; 25(2): 392–401. [PubMed: 17038674]
10. Sottile V, Thomson A, McWhir J. In vitro osteogenic differentiation of human ES cells. Cloning Stem Cells. 2003; 5(2):149–55. [PubMed: 12930627]
11. Lavon N, Yanuka O, Benvenisty N. Differentiation and isolation of hepatic-like cells from human embryonic stem cells. Differentiation. 2004; 72(5):230–8. [PubMed: 15270779]
12. Segev H, et al. Differentiation of human embryonic stem cells into insulin-producing clusters. Stem Cells. 2004; 22(3):265–74. [PubMed: 15153604]
13. Green H, Easley K, Iuchi S. Marker succession during the development of keratinocytes from cultured human embryonic stem cells. Proc Natl Acad Sci U S A. 2003; 100(26):15625–30. [PubMed: 14663151]
14. Li Z, et al. Differentiation, survival, and function of embryonic stem cell-derived endothelial cells for ischemic heart disease. Circulation. 2007; 116(11):I46–54. [PubMed: 17846325]

15. Drukker M, et al. Human embryonic stem cells and their differentiated derivatives are less susceptible to immune rejection than adult cells. Stem Cells. 2006; 24(2):221–9. [PubMed: 16109762]
16. Wang ZZ, et al. Endothelial cells derived from human embryonic stem cells form durable blood vessels in vivo. Nat Biotechnol. 2007; 25(3):317–8. [PubMed: 17322871]
17. Chiu RC. Bone-marrow stem cells as a source for cell therapy. Heart Fail Rev. 2003; 8(3):247–51. [PubMed: 12878833]
18. Cao F, et al. In vivo visualization of embryonic stem cell survival, proliferation, and migration after cardiac delivery. Circulation. 2006; 113(7):1005–14. [PubMed: 16476845]
19. Suzuki Y, et al. In vitro comparison of the biological effects of three transfection methods for magnetically labeling mouse embryonic stem cells with ferumoxides. Magn Reson Med. 2007; 57(6):1173–9. [PubMed: 17534917]
20. Suzuki Y, Yeung AC, Yang PC. Cardiovascular MRI for stem cell therapy. Curr Cardiol Rep. 2007; 9(1):45–50. [PubMed: 17362684]
21. Stuckey DJ, et al. Iron particles for noninvasive monitoring of bone marrow stromal cell engraftment into, and isolation of viable engrafted donor cells from, the heart. Stem Cells. 2006; 24(8):1968–75. [PubMed: 16627684]
22. Cunningham CH, et al. Positive contrast magnetic resonance imaging of cells labeled with magnetic nanoparticles. Magn Reson Med. 2005; 53(5):999–1005. [PubMed: 15844142]
23. Xu C, et al. Feeder-free growth of undifferentiated human embryonic stem cells. Nat Biotechnol. 2001; 19(10):971–4. [PubMed: 11581665]
24. Yamashita J, et al. Flk1-positive cells derived from embryonic stem cells serve as vascular progenitors. Nature. 2000; 408(6808):92–6. [PubMed: 11081514]
25. Arbab AS, et al. Magnetic resonance imaging and confocal microscopy studies of magnetically labeled endothelial progenitor cells trafficking to sites of tumor angiogenesis. Stem Cells. 2006; 24(3):671–8. [PubMed: 16179427]
26. McCloskey KE, et al. Purified and proliferating endothelial cells derived and expanded in vitro from embryonic stem cells. Endothelium. 2003; 10(6):329–36. [PubMed: 14741848]
27. Rosenzweig A. Endothelial progenitor cells. N Engl J Med. 2003; 348(7):581–2. [PubMed: 12584365]
28. Wu JC, et al. Proteomic analysis of reporter genes for molecular imaging of transplanted embryonic stem cells. Proteomics. 2006; 6(23):6234–49. [PubMed: 17080479]
29. Wu JC, et al. Transcriptional profiling of reporter genes used for molecular imaging of embryonic stem cell transplantation. Physiol Genomics. 2006; 25(1):29–38. [PubMed: 16390873]
30. Voyta JC, et al. Identification and isolation of endothelial cells based on their increased uptake of acetylated-low density lipoprotein. J Cell Biol. 1984; 99(6):2034–40. [PubMed: 6501412]
31. Himes N, et al. In vivo MRI of embryonic stem cells in a mouse model of myocardial infarction. Magn Reson Med. 2004; 52(5):1214–9. [PubMed: 15508153]
32. Kraitchman DL, et al. In vivo magnetic resonance imaging of mesenchymal stem cells in myocardial infarction. Circulation. 2003; 107(18):2290–3. [PubMed: 12732608]
33. Guzman R, et al. Long-term monitoring of transplanted human neural stem cells in developmental and pathological contexts with MRI. Proc Natl Acad Sci U S A. 2007; 104(24):10211–6. [PubMed: 17553967]
34. Cao F, et al. Molecular imaging of embryonic stem cell misbehavior and suicide gene ablation. Cloning Stem Cells. 2007; 9(1):107–17. [PubMed: 17386018]
35. Reinecke H, Murry CE. Taking the death toll after cardiomyocyte grafting: a reminder of the importance of quantitative biology. J Mol Cell Cardiol. 2002; 34(3):251–3. [PubMed: 11945017]
36. Chang GY, Xie X, Wu JC. Overview of stem cells and imaging modalities for cardiovascular diseases. J Nucl Cardiol. 2006; 13(4):554–69. [PubMed: 16919579]
37. Levenberg S, et al. Engineering vascularized skeletal muscle tissue. Nat Biotechnol. 2005; 23(7): 879–84. [PubMed: 15965465]
38. Kajstura J, et al. Endothelial progenitor cells: neovascularization or more? J Mol Cell Cardiol. 2006; 40(1):1–8. [PubMed: 16321397]

39. Laflamme MA, et al. Cardiomyocytes derived from human embryonic stem cells in pro-survival factors enhance function of infarcted rat hearts. Nat Biotechnol. 2007; 25(9):1015–1024. [PubMed: 17721512]

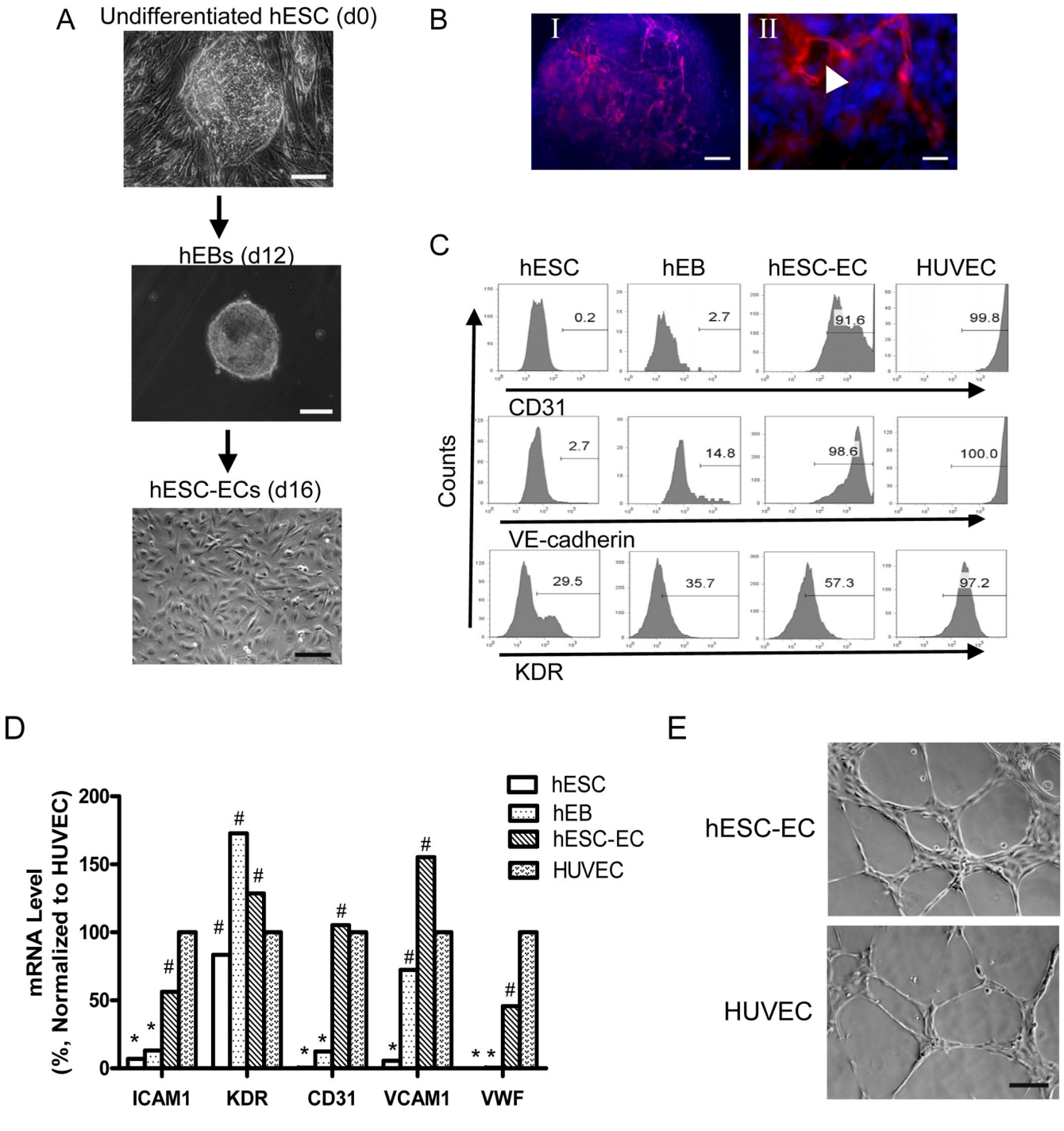

Figure 1. *In vitro* endothelial differentiation of hES cells

(A) Schematic outline of the differentiation procedures. Undifferentiated hES cells were grown to 60%–70% confluence on mouse embryonic fibroblasts (MEFs) or on Matrigel in MEF conditioned medium, dated as day 0. At day 12, hEBs were collected and digested by Liberase Blendzyme IV and $CD31^+$ cells were isolated by FACS and sub-cultured in EGM-2 medium to expand and induce endothelial maturation. Scale bar=20μm (upper and lower) and 100μm (middle). **(B)** Whole-mount immunochemistry of day-12 hEB. Areas of CD31 cells (red) within hEBs are organized in elongated clusters (I) and channels (II,

arrowhead). Cell nuclei stained with DAPI (blue). Scale bar=50μm (I) and 10μm (II)**. (C)** Flow cytometric analysis of endothelial cell markers (CD31, VE-cadherin, and KDR). Percent positive cells are shown. hESC-ECs were isolated from day-12 hEB by FACSan and subcultured. HUVECs were used as positive control. Isotype-matched antibodies were used in flow cytometry for background fluorescence. **(D)** Comparison of mRNA expression levels of hESC, hEB and hESC-EC between HUVEC. The quantification was performed by real-time RT-PCR. Experiments were performed in triplicates. $^{\#}P>0.05$, $*P<0.05$ compared to HUVEC. **(E)** Endothelial tube formation by hESC-ECs and HUVECs after 12 hours of plating on Matrigel in 24-well plates. Scale bar=20μm. Abbreviations: hEB, human embryoid body; hESC, human ES cell; FACS, fluorescence activated cell sorting; HUVEC, human umbilical vein endothelial cell.

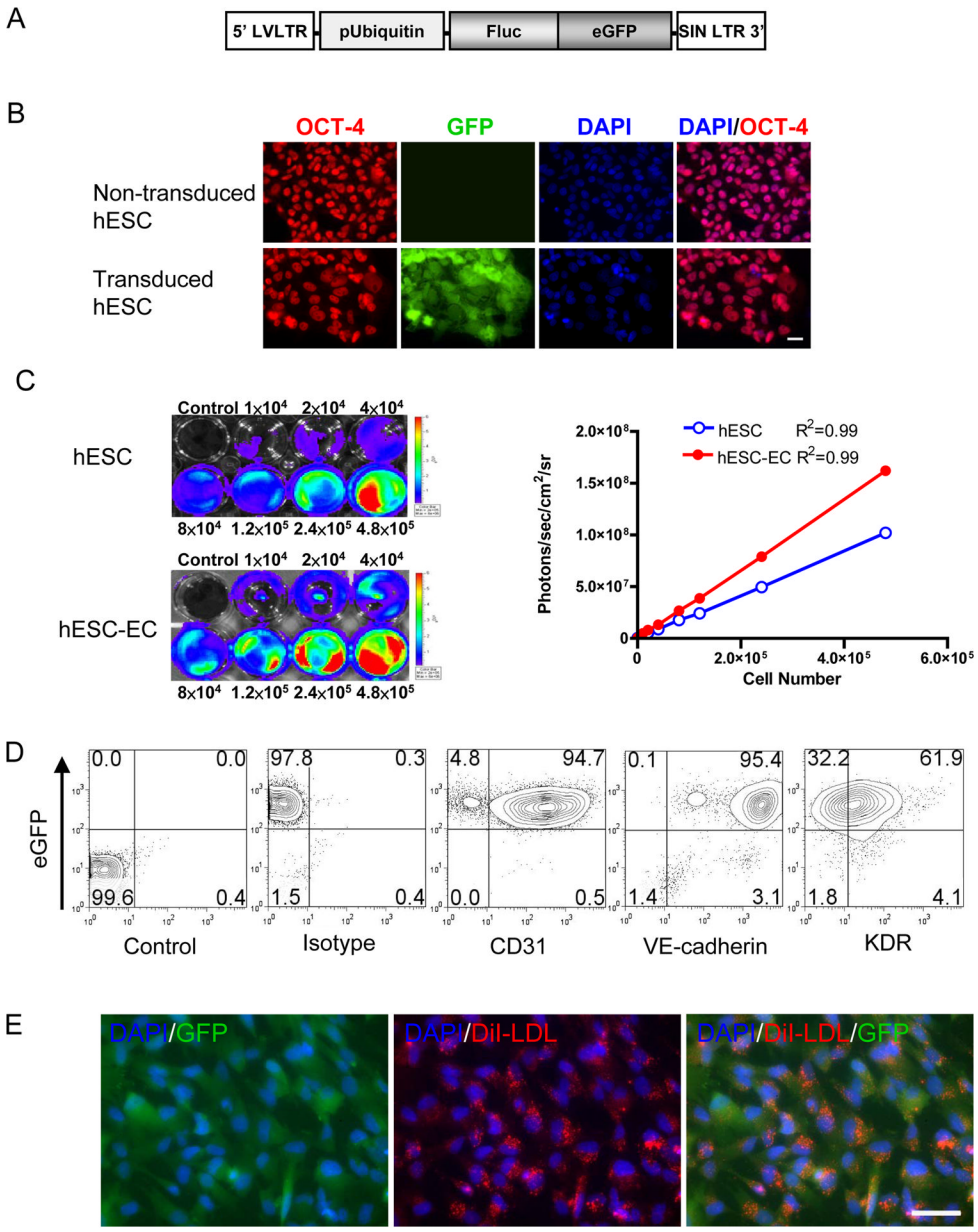

Figure 2. Stable lentiviral transduction of hES cells with the double fusion reporter genes

(A) Schema of the double fusion reporter gene containing fusion of Fluc-eGFP. The double fusion reporter gene was cloned into a self-inactivating lentiviral vector downstream from the constitutive ubiquitin promoter. **(B)** Control nontransduced hES cells and transduced hES cells showed similar expression pattern of Oct-4 under fluorescence microscopy. DAPI staining is used as a nuclear marker. Scale bar=10μm. **(C)** *Ex vivo* imaging analysis of stably transduced hES cells show increasing bioluminescence signals with cell numbers of hES cells (r^2=0.99) and with hESC-ECs (r^2=0.99). Compared to hES cells, hESC-ECs expressed higher bioluminescence activity. Data are representative of three independent experiments. **(D)** Flow cytometric analysis of double fusion hESC-ECs. Percent positive cells are shown in upper right hand corner. Double fusion hESC-ECs were isolated from day-12 hEB by FACSan and subcultured. Normal hESC-ECs were used as control. Isotype-matched antibodies were used in flow cytometry for background fluorescence. **(E)** Uptake of

DiI-ac-LDL (red) by double fusion hESC-ECs. Nuclei were stained with DAPI (blue). Data are representative of three independent experiments. Scale bar=50μm. Abbreviations: DAPI, 4′, 6-diamidino-2-phenylindole; EC, endothelial cell; LDL, low density lipoprotein.

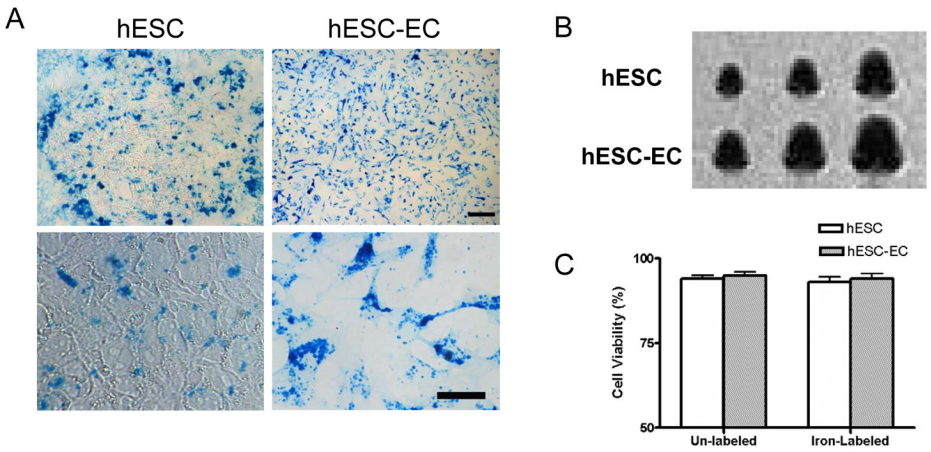

Figure 3. Iron particle labeling of hES cells and hESC-ECs

(A) Prussian blue staining for iron shows cytosolic deposition of blue crystals. Upper panel is 100X and lower panel is 1000X magnification. Scale bar=100μm (upper) and 10μm (lower). **(B)** Representative *in vitro* cellular MR images. Iron-labeled hESC-ECs demonstrated larger area of signal dephasing. The cell suspensions in 96-well plates each contain 1×10^4, 5×10^4, 1×10^5 iron-labeled cells (from left to right). **(C)** Trypan blue cell viability assay show no significant difference between control unlabeled cells and iron labeled cells for both cell populations (hESC and hESC-EC).

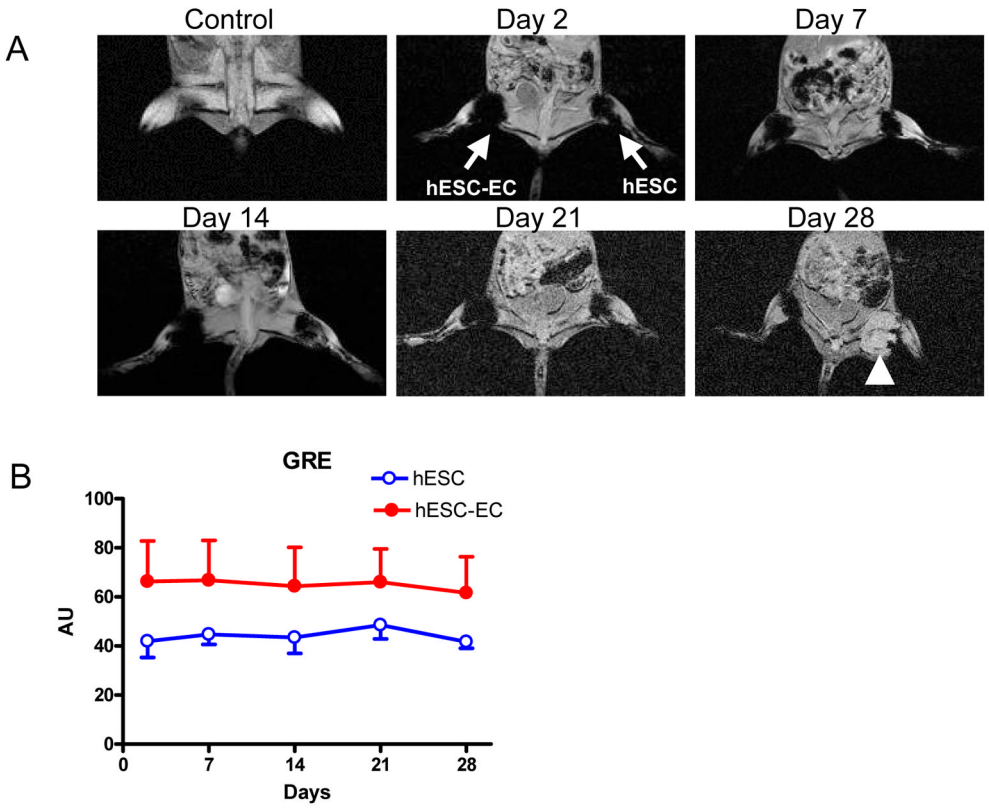

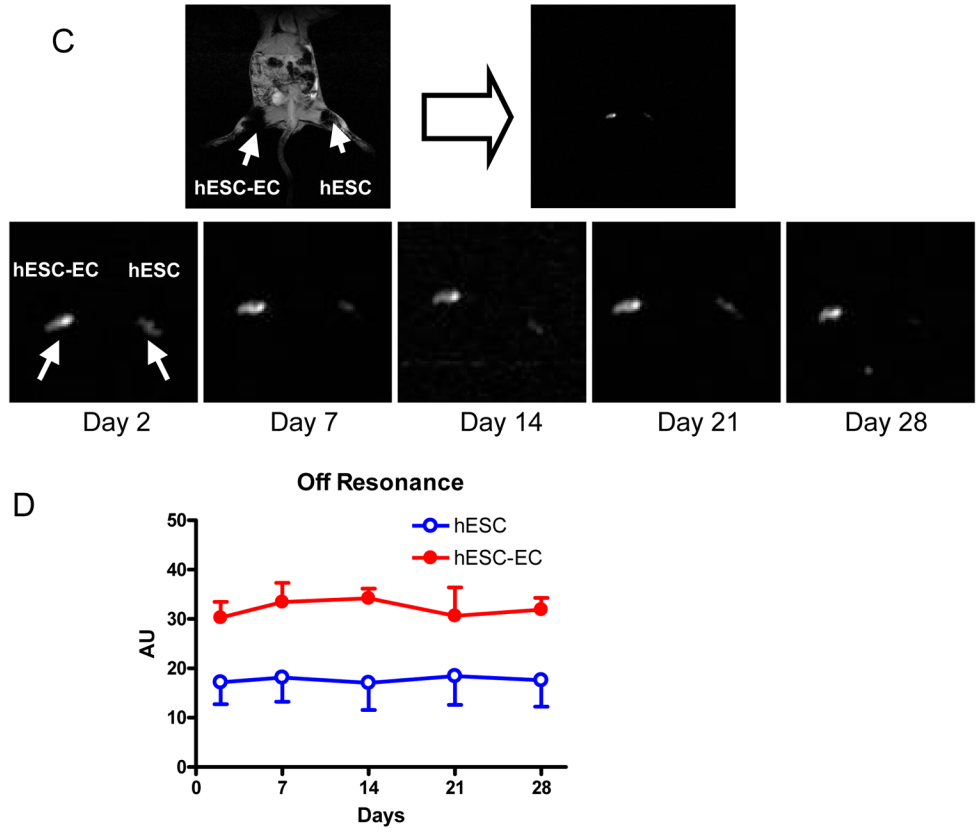

Figure 4. Serial *in vivo* MR imaging of iron-labeled cells from day 2 to week 4

(A) Representative *in vivo* gradient-recalled echo (GRE) imaging. No hypointense signal is found in the MR image of control mouse injected with unlabeled cells. MR signals showed no significant difference from day 2 to day 28. MR image by GRE at day 28 shows bulking expansion of the left hind limb injected with hES cells due to teratoma formation (arrow head). **(B)** Detailed quantitative analysis of GRE signals from all animals transplanted with hES cells and hESC-ECs (signal activity is expressed as authority unit (AU)). **(C)** Representative *in vivo* Off-Resonance (OR) imaging. **(D)** The analysis of quantitative OR signal from all animals transplanted with iron-labeled cells. No significant differences in the OR signal analysis was observed from day 2 to day 28. Abbreviations: GRE, gradient-recalled echo; OR, off-resonance.

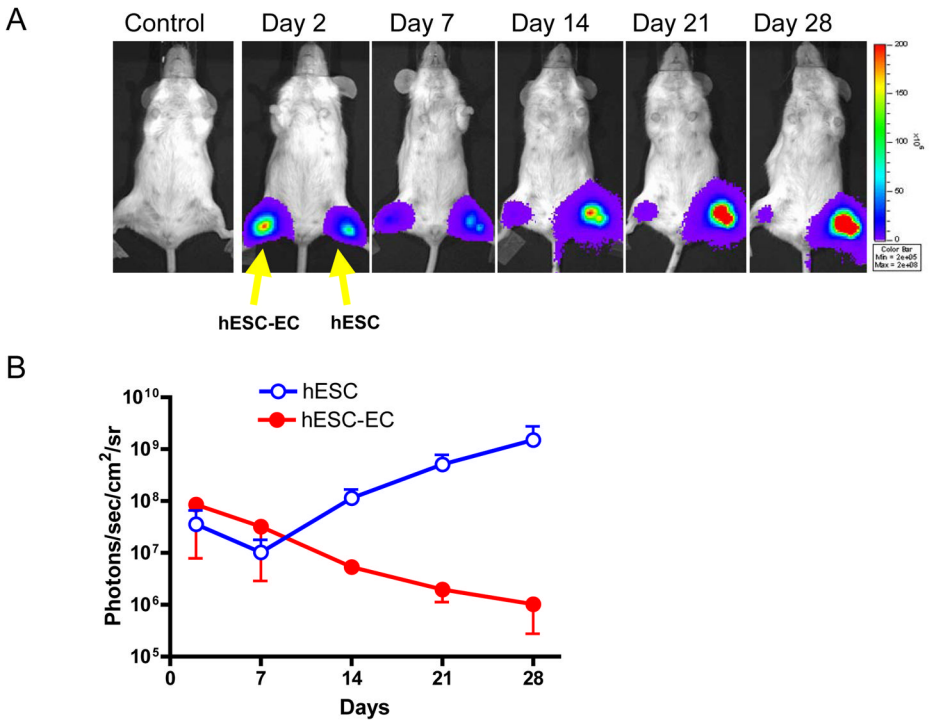

Figure 5. Reporter gene imaging of hES cell and hESC-EC fate after transplantation

(A) A representative animal injected with 1×10^6 hESC-ECs (right hind limb) shows significant bioluminescence activity at day 2, which decreases progressively over the following 4 weeks. In contrast, undifferentiated hES cells (left hind limb) show the lowest bioluminescence signals at day 7, which increases dramatically during week 2 and week 4. **(B)** Detailed quantitative analysis of signals from all animals transplanted with hES cells versus hESC-ECs. Signal activity is expressed as photons/sec/cm^2/sr. Note the Y-axis is shown as log 10 scale.

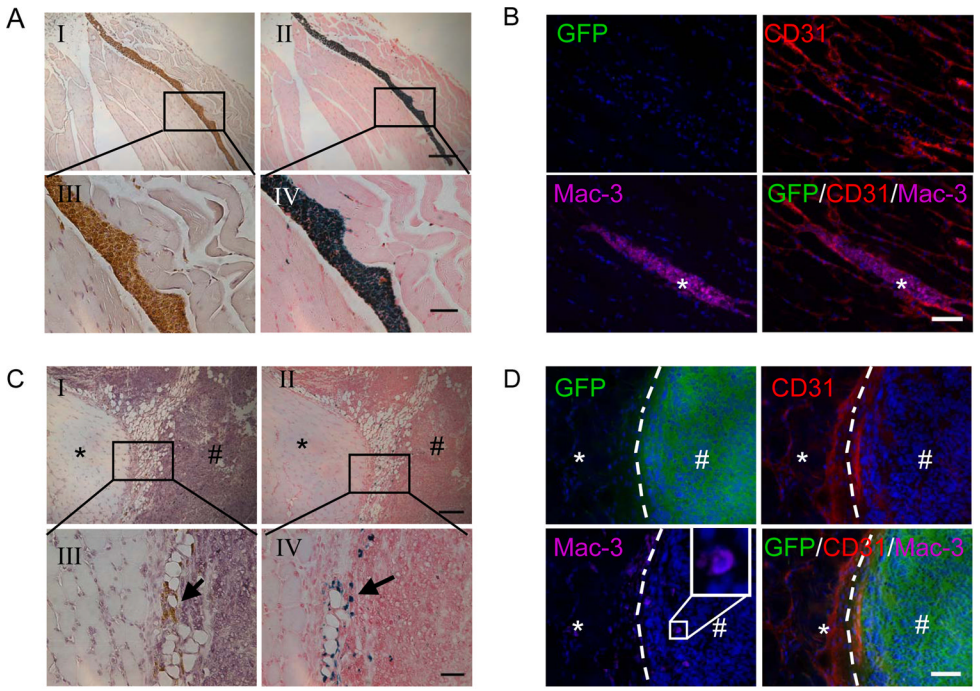

Figure 6. Histologic analysis of double labeled hES cells and hESC-ECs

(A) Staining for macrophages and iron 4 weeks after transplantation of hESC-ECs. Immunostaining of Mac-3 for macrophages (I, III) and Prussian blue for iron (II, IV) were counterstained with hematoxylin and nuclear fast red, respectively. Note macrophages loaded with iron particles can be found in between muscle bundles. Scale bar=100μm (I, III) and 20μm (II, IV). **(B)** Immunofluorescence staining of GFP for transplanted double fusion hESC-ECs, CD31 for microvasculature of hindlimb, and Mac-3 for macrophages at 4 weeks after transplantation. There were no transplanted GFP^+ hESC-ECs found nearby macrophages. Nuclei were stained with DAPI (blue). Scale bar=20μm. **(C)** Staining for macrophages and iron 4 weeks after implantation of undifferentiated hES cells. Prussian blue positive cells are distributed between normal skeletal muscles (*) and teratoma (#). Scale bar=100μm (I, III) and 20μm (II, IV). **(D)** Immunofluorescence staining for GFP, CD31 and macrophages 4 weeks after transplantation of hESCs. GFP staining showed teratoma formation (#) and clear edge (dashed line) separating from the normal muscle fibers (*). Nuclei were stained with DAPI (blue). Scale bar= 20μm.